EPR of Gd^{3+} in a single crystal of thorium oxysulfide

G. Amoretti, D. C. Giori, and V. Varacca
Gruppo Nazionale di Struttura della Materia del Consiglio Nazionale delle Ricerche, Istituto di Fisica dell'Università, Parma, Italy

J. C. Spirlet and J. Rebizant
Commission of the European Communities, Joint Research Center, Karlsruhe Establishment, European Institute for Transuranium Elements, Postfach 2266, D-7500 Karlsruhe, Federal Republic of Germany

(Received 16 April 1979)

The electron paramagnetic resonance of Gd^{3+} has been studied in a single crystal of thorium oxysulfide. The experimental results are interpreted using a spin Hamiltonian for tetragonal symmetry, and the crystal-field parameters and the g factor are determined. The very good agreement between the calculated and experimental data shows that the Gd^{3+} ion enters substitutionally, and that the charge compensation is far enough away to avoid any distortion of the local symmetry.

I. INTRODUCTION

The paramagnetic resonance studies of S-state ions in host crystals are of interest for two fundamental reasons: (a) the possibility of a detailed determination of the character of the crystal field acting on the ion and therefore the knowledge of the site symmetry at the location of the ion; (b) the information that one can obtain on the mechanism which governs the zero-field splittings of the ground state. In this regard, it has been shown[1] that a purely ionic model is inadequate to explain the experimental results and that a certain amount of covalency with the ligands, induced by spin-orbit coupling, must be considered.[2,3]

This paper deals principally with point (a) and describes the theoretical and experimental machinery used to obtain the crystal-field data.

II. CRYSTAL GROWTH AND CHARACTERIZATION

Single crystals of actinide chalcogenides with well developed natural faces and low defect density can be grown by chemical transport reaction using iodine as transporting agent.[4] The mechanism of the process is described in Fig. 1.

Gadolinium-doped thorium oxysulfide (ThOS) single crystals were obtained by this method. The transport reaction is carried out in quartz bulbs (25 mm in diameter and 150 mm long) in a temperature gradient furnace. The gadolinium-doped ThOS powder (5 g, with a gadolinium concentration of the order of 500 ppm) is introduced into the carefully cleaned bulbs with a quantity of iodine sufficient to produce a pressure of 2 atmospheres at 900 °C. The quartz bulb is evacuated and sealed under a pressure of 10^{-6} Torr. The transport process occurs in a temperature gradient of 50 °C. The crystals grow at 850 °C maintaining the feed power at 900 °C.

After two weeks, 2-mm-long transparent platelets are obtained. The crystals were characterized by x-ray diffraction methods. The rotating crystal photograph and the Debye-Scherrer pattern reveal a tetragonal structure (space group $P4/nmm$) with lattice parameters

$$a = 3.973 \pm 0.004 \text{ Å} ,$$

$$c = 6.773 \pm 0.008 \text{ Å} ,$$

in agreement with published data.[5] The quality of the Laue pattern (Fig. 2) is an indication of the high level of perfection of the crystals. From the symmetry and the intensity of the EPR spectrum it is evident that the doping Gd^{3+} ions enter substitutionally and in a proportion of the order of 10 ppm.

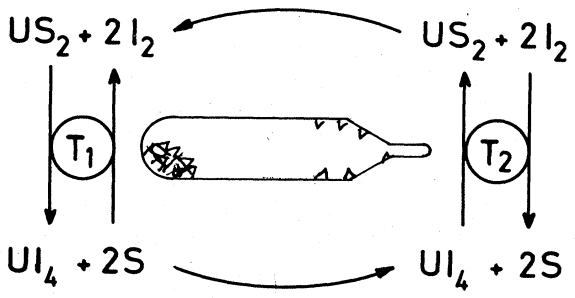

FIG. 1. Chemical transport process of chalcogenides in a closed system; T_1 and T_2 are, respectively, the feed and the growth temperatures ($T_1 > T_2$).

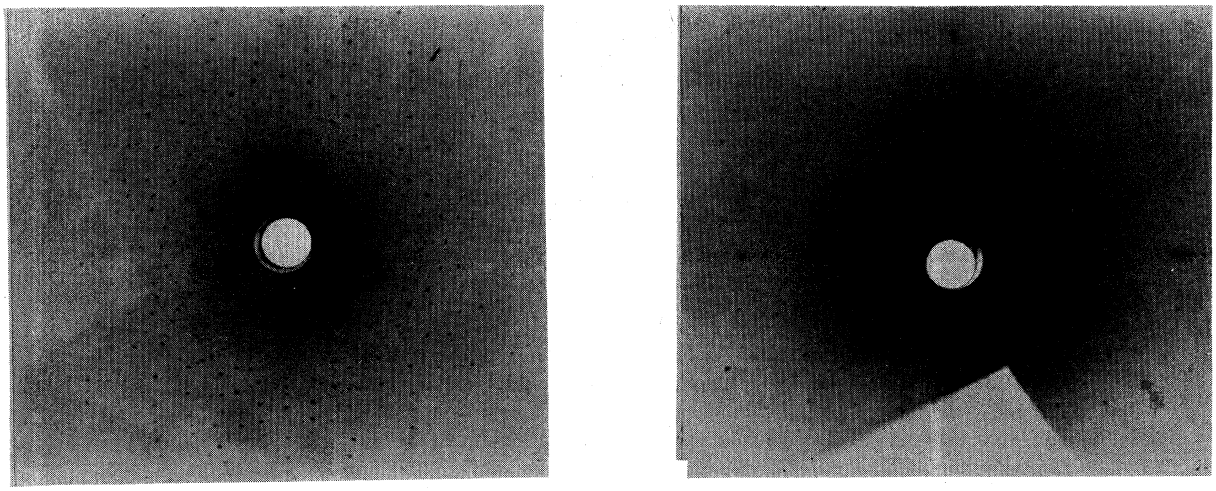

FIG. 2. (a) Transmission and (b) back-reflection photograph of ThOS single crystal. The incident beam is perpendicular to the (001) plane (30-mm specimen-to-film distance).

III. THEORY

The ground state of the Gd^{3+} ion is essentially $^8S_{7/2}$. The EPR spectra reproduce the tetragonal symmetry of the Th crystal site (point group C_{4v}). Therefore, the spin Hamiltonian for the magnetic field parallel to the crystal-field z axis can be written

$$\mathcal{H} = g_{\parallel}\mu_B H_z S_z + B_2^0 O_2^0 + B_4^0 O_4^0 + B_6^0 O_6^0 + B_4^4 O_4^4 + B_6^4 O_6^4 \ , \tag{1}$$

where μ_B is the Bohr magneton, the B_n^m's are the crystal-field parameters, and the O_n^m's are the corresponding operators with matrix elements proportional to those of the related spherical harmonics.[6]

When H is placed along the x (or y) axis, the Hamiltonian (1) transforms to the following, obtained by projection, in the usual way, on the new axes,[7]

$$\mathcal{H} = g_{\perp}\mu_B H S_{z'} + C_2^0 O_2^0 + C_4^0 O_4^0 + C_6^0 O_6^0 + C_2^2 O_2^2 + C_4^2 O_4^2 + C_4^4 O_4^4 + C_6^2 O_6^2 + C_6^4 O_6^4 + C_6^6 O_6^6 \ , \tag{2}$$

where the coefficients C_n^m's are related to the B_n^m's as follows:

$$C_2^0 = -\tfrac{1}{2}B_2^0, \quad C_4^0 = \tfrac{1}{8}(3B_4^0 + B_4^4) \ , \quad C_6^0 = -\tfrac{1}{16}(5B_6^0 + B_6^4), \quad C_2^2 = \tfrac{3}{2}B_2^0 \ ,$$

$$C_4^2 = -\tfrac{1}{2}(5B_4^0 - B_4^4), \quad C_4^4 = \tfrac{1}{8}(35B_4^0 + B_4^4) \ , \quad C_6^2 = \tfrac{1}{32}(105B_6^0 + 5B_6^4), \quad C_6^4 = -\tfrac{1}{16}(63B_6^0 - 13B_6^4) \ ,$$

$$C_6^6 = \tfrac{1}{32}(231B_6^0 + 11B_6^4) \ . \tag{3}$$

As usual, instead of the B_n^m's, we will use in the following the reduced parameters b_n^m, defined as

$$b_2^m = 3B_2^m, \quad b_4^m = 60B_4^m, \quad b_6^m = 1260B_6^m \ , \tag{4}$$

and therefore also the parameters c_n^m, related in the same way to the C_n^m's.

From Eqs. (1) and (2) we obtain, with a perturbative procedure up to the third order, the following general scheme [Eqs. (5)] for the seven lines of the EPR spectrum, where the P_i's and H_0 are given in Table I.

$$H_1 = H_0 + (P_1 - P_2) - \frac{1}{4H_1}(2P_6^2 + P_7^2 - P_8^2 - 2P_9^2)$$

$$- \frac{1}{4H_1^2}[\tfrac{2}{9}P_5^2(P_1 - P_2) + P_6^2(P_1 - P_3) + \tfrac{1}{4}P_7^2(P_1 - P_4) - \tfrac{1}{4}P_8^2(P_2 - P_3) - P_9^2(P_2 - P_4)$$

$$- \tfrac{1}{3}P_5(P_6P_8 - P_7P_9) - P_{10}(P_6P_7 - P_8P_9)] \ , \tag{5a}$$

TABLE I. Values of the parameters P_i and H_0 for Eqs. (5).

	$\vec{H}_{\parallel}\vec{z}$	$\vec{H}_{\parallel}\vec{x}$
P_1	$\frac{1}{g_{\parallel}\mu_B}(7b_2^0+7b_4^0+b_6^0)$	$\frac{1}{g_{\perp}\mu_B}(7c_2^0+7c_4^0+c_6^0)$
P_2	$\frac{1}{g_{\parallel}\mu_B}(b_2^0-13b_4^0-5b_6^0)$	$\frac{1}{g_{\perp}\mu_B}(c_2^0-13c_4^0-5c_6^0)$
P_3	$\frac{1}{g_{\parallel}\mu_B}(-3b_2^0-3b_4^0+9b_6^0)$	$\frac{1}{g_{\perp}\mu_B}(-3c_2^0-3c_4^0+9c_6^0)$
P_4	$\frac{1}{g_{\parallel}\mu_B}(-5b_2^0+9b_4^0-5b_6^0)$	$\frac{1}{g_{\perp}\mu_B}(-5c_2^0+9c_4^0-5c_6^0)$
P_5	0	$\frac{1}{g_{\perp}\mu_B}\frac{2c_6^6}{\sqrt{7}}$
P_6	0	$\frac{1}{g_{\perp}\mu_B}\left(\frac{21^{1/2}}{3}c_2^2+\frac{21^{1/2}}{2}c_4^2+\frac{2}{21^{1/2}}c_6^2\right)$
P_7	$\frac{1}{g_{\parallel}\mu_B}[(\frac{7}{5})^{1/2}b_4^4+(\frac{5}{7})^{1/2}b_6^4]$	$\frac{1}{g_{\perp}\mu_B}[(\frac{7}{5})^{1/2}c_4^4+(\frac{5}{7})^{1/2}c_6^4]$
P_8	$\frac{1}{g_{\parallel}\mu_B}\left(\sqrt{3}b_4^4-\frac{1}{\sqrt{3}}b_6^4\right)$	$\frac{1}{g_{\perp}\mu_B}\left(\sqrt{3}c_4^4-\frac{1}{\sqrt{3}}c_6^4\right)$
P_9	0	$\frac{1}{g_{\perp}\mu_B}\left(\sqrt{5}c_2^2+\frac{1}{2\sqrt{5}}c_4^2-\frac{2}{\sqrt{5}}c_6^2\right)$
P_{10}	0	$\frac{1}{g_{\perp}\mu_B}\left(2(\frac{5}{3})^{1/2}c_2^2-2(\frac{3}{5})^{1/2}c_4^2+\frac{2}{15^{1/2}}c_6^2\right)$
H_0	$\frac{h\nu}{g_{\parallel}\mu_B}$	$\frac{h\nu}{g_{\perp}\mu_B}$

$$H_2=H_0+(P_2-P_3)-\frac{1}{6H_2}(P_5^2+3P_6^2+3P_9^2-3P_{10}^2)$$
$$-\frac{1}{4H_2^2}[-\tfrac{1}{9}P_5^2(P_1-P_2)+P_6^2(P_1-P_3)+\tfrac{1}{2}P_8^2(P_2-P_3)+P_9^2(P_2-P_4)$$
$$-P_{10}^2(P_3-P_4)-\tfrac{2}{3}P_5(2P_6P_8+P_7P_9)-2P_{10}P_6P_7]\ , \tag{5b}$$

$$H_3=H_0+(P_3-P_4)-\frac{1}{4H_3}(-2P_6^2-P_7^2+P_8^2+2P_9^2)$$
$$-\frac{1}{4H_3^2}[-P_6^2(P_1-P_3)+\tfrac{1}{4}P_7^2(P_1-P_4)-\tfrac{1}{4}P_8^2(P_2-P_3)+P_9^2(P_2-P_4)$$
$$+2P_{10}^2(P_3-P_4)+P_5(P_6P_8-P_7P_9)+3P_{10}(P_6P_7-P_8P_9)]\ , \tag{5c}$$

$$H_4=H_0-\frac{1}{2H_4}(P_7^2-2P_9^2+2P_{10}^2)\ , \tag{5d}$$

$$H_5=H_0-(P_3-P_4)-\frac{1}{4H_5}(-2P_6^2-P_7^2+P_8^2+2P_9^2)$$
$$+\frac{1}{4H_5^2}[-P_6^2(P_1-P_3)+\tfrac{1}{4}P_7^2(P_1-P_4)-\tfrac{1}{4}P_8^2(P_2-P_3)+P_9^2(P_2-P_4)$$
$$+2P_{10}^2(P_3-P_4)+P_5(P_6P_8-P_7P_9)+3P_{10}(P_6P_7-P_8P_9)]\ , \tag{5e}$$

$$H_6 = H_0 - (P_2 - P_3) - \frac{1}{6H_6}(P_5^2 + 3P_6^2 + 3P_9^2 - 3P_{10}^2)$$
$$+ \frac{1}{4H_6^2}[-\tfrac{1}{9}P_5^2(P_1 - P_2) + P_6^2(P_1 - P_3) + \tfrac{1}{2}P_8^2(P_2 - P_3) + P_9^2(P_2 - P_4)$$
$$- P_{10}^2(P_3 - P_4) - \tfrac{2}{3}P_5(2P_6P_8 + P_7P_9) - 2P_{10}P_6P_7] \ , \quad (5f)$$

$$H_7 = H_0 - (P_1 - P_2) - \frac{1}{4H_7}(2P_6^2 + P_7^2 - P_8^2 - 2P_9^2)$$
$$+ \frac{1}{4H_7^2}[\tfrac{2}{9}P_5^2(P_1 - P_2) + P_6^2(P_1 - P_3) + \tfrac{1}{4}P_7^2(P_1 - P_4) - \tfrac{1}{4}P_8^2(P_2 - P_3)$$
$$- P_9^2(P_2 - P_4) - \tfrac{1}{3}P_5(P_6P_8 - P_7P_9) - P_{10}(P_6P_7 - P_8P_9)] \ . \quad (5g)$$

It is to be noted that the third order of perturbation is more than enough to describe the parallel spectrum. In fact, the third-order terms are smaller than the experimental uncertainty on the determination of the field position of the lines. The situation is different in the perpendicular case. In fact, owing to the large contributions of the terms in c_2^0 and c_2^2, the third-order terms are not negligible in this case. Therefore, the values of the crystal-field parameters, obtained by fitting the perpendicular spectrum with Eqs. (5), require an ulterior refinement.[8]

IV. EXPERIMENTAL

The spectra have been recorded by means of a modified *X*-band Varian 9*E*-line spectrometer. In particular, for each line of the spectra, the field position was measured as follows: the magnetic field was set to a value very close to the position of the line by means of the Varian Fieldial, calibrated by comparison with a Bruker BH12 nuclear resonance probe, coupled to a Hewlett-Packard 5245L frequency counter. Then, the field was increased step by step with a suitable device,[9] while the derivative of the EPR absorption was monitored on a chart recorder. The number of steps (each corresponding to a constant increment ΔH), necessary to reach the inversion point of the derivative, and the reading of the Fieldial gave the field position of the line. In this way, we have obtained a sensitivity better than 0.1 G for lines of ~15 G of width. This procedure was made easier by the fact that no hyperfine structure was observed. In the same way the resonance field was measaured for a sample of DPPH (α, α', -diphenyl-β-picrylhydrazyl), placed inside the E233 rotating cavity together with the crystal, which allows one to obtain the microwave frequency, using its g value of 2.00368 ±0.00005, as measured with our equipment.

The crystal was placed rigidly inside a plexiglas capsule, which was fixed to a rod inserted into the cavity. The orientation of the principal symmetry axes of the crystal field was determined following the angular variation of the spectrum in three mutually orthogonal planes, the first of which was (001). Such determination has an uncertainty smaller than 1°, and the consequent possible error in the field position of the lines is less than the instrumental one. However, taking into account all the possible error sources, the final uncertainty on the values of the measured field positions is not greater than ±0.4 gauss.

The z axis is the direction for which the spectrum shows the maximum overall splitting (about 2300 G from the data of Table II) and coincides with the [001] axis. In the perpendicular plane, we have assumed, as usual, the x and y axes in correspondence to the equivalent positions of maximum splitting (about 1350 G, see again Table II). An alternative choice is the positions of minimum splitting. In such a case one would obtain the opposite signs for the parameters b_4^4 and b_6^4, responsible for the $\frac{1}{2}\pi$ symmetry of the spectrum in the xy plane, but the same absolute value.

TABLE II. Fitting of the field positions (in gauss) of the lines, for the parallel and perpendicular spectra, obtained with the parameters of Table III.

$\vec{H} \parallel \vec{z}$		$\vec{H} \parallel \vec{x}$	
H_{exp}	H_{calc}	H_{exp}	H_{calc}
2076.1	2076.7	2588.0	2587.9
2428.2	2428.6	2890.8	2890.4
2801.4	2801.2	3040.9	3040.5
3227.1	3226.5	3171.3	3171.0
3652.0	3651.8	3336.1	3336.3
4024.7	4024.8	3560.3	3560.8
4376.8	4377.0	3941.5	3942.1

TABLE III. g values and crystal-field parameters (in units of 10^{-4} cm^{-1}) for Gd^{3+} in ThOS.

$g_{\parallel}$	$g_{\perp}$	b_2^0	b_4^0	b_6^0	b_4^4	b_6^4
1.9915 ±0.0003	1.9911 ±0.0003	−183.33 ±0.02	1.704 ±0.006	−0.591 ±0.008	28.30 ±0.05	−4.76 ±0.13

V. FITTING PROCEDURE

The b_n^0 parameters are well determined by fitting Eqs. (5) with the experimental values of the parallel spectrum. A good value of $g_{\parallel}$ is also obtained in this case. At the same time, a first approximation for the values of the b_n^m's and $g_{\perp}$ is obtained from the perpendicular spectrum. This was performed by means of an iterative procedure on two systems of linear equations built up from Eqs. (5). Essentially, we evaluate $g_{\parallel}$ and the b_n^0's from the four equations obtained, for the parallel case, from H_4 and the differences $H_1 - H_7$, $H_2 - H_6$, and $H_3 - H_5$, in which we neglect, in the first step, the terms of second and third order. The same is made, in the perpendicular case, for $g_{\perp}$ and the c_n^0's. From these values of the b_n^0's and c_n^0's, by means of Eq. (3), we obtain the values of the b_n^m's, which are used, in the second step, to correct the equations with the terms previously dropped. Such corrections are successively repeated until an adequated consistency is reached. The values of the parameters obtained in this way are then used as starting values for a trial and error procedure in which the energy matrices of the Hamiltonians (1) and (2) are exactly diagonalized.[10] As said, the values of the b_n^0's and $g_{\parallel}$ remain practically unchanged in this refinement. The final values of the spin-Hamiltonian parameters are shown in Table III, while in Table II we report, for comparison, the experimental and calculated values of the fields (obtained with the parameters of Table III), for the parallel and perpendicular spectra. The precision of the fitting, as evident from Table II, is supported also by the coincidence, inside the quoted uncertainty, of the value of b_2^0 obtained from the "parallel" equations with that deduced from c_2^0 in the perpendicular case.

The signs of the parameters of Table III are relative only, because the absolute signs depend on which state ($+\frac{7}{2}$ or $-\frac{7}{2}$) is the lowest in energy (and, for b_4^4 and b_6^4, also on the choice of the x and y axes). We have in mind to make measurements at liquid-helium temperature, because a comparison of the relative intensity of the lines at room-temperature and liquid-helium temperatures can give the sign of b_2^0 and therefore of the other b_n^0's.[11]

VI. DISCUSSION

The perfect tetragonality of the crystal field confirms that the Gd^{3+} ion enters substitutionally at the Th^{4+} site. Moreover, the absence of distortions shows that the charge compensation due to the different valence of the two ions is not in the neighbors of the doping ion and is probably connected with some surface defect.

The g factor is practically isotropic, as expected for an $^8S_{7/2}$ ion. Its value is slightly smaller than the calculated 1.9928,[1,3] and this may be attributed to covalency effects, taking also into account that O is a ligand which usually shows a high covalency degree. This is consistent with the relatively low absolute value of b_2^0 (one of the smallest for tetragonal symmetry[12]), which may be due both to a smaller than usual excited-states spin-orbit admixture (and this would lead to a greater value for the calculated g factor) and to a reduction of the ligand field effects produced by a certain amount of covalency.

ACKNOWLEDGMENTS

We wish to thank Dr. G. Calestani for his assistance in the sample preparation and Mr. B. Valenti for his help in recording the spectra.

[1]B. G. Wybourne, Phys. Rev. 148, 317 (1966).
[2]D. J. Newman and M. M. Ellis, Phys. Lett. 23, 46 (1966).
[3]D. J. Newman and W. Urban, Adv. Phys. 24, 793 (1975).
[4]J. C. Spirlet, J. Phys. (Paris) (to be published).
[5]W. H. Zachariasen, Acta Crystallogr. 2, 291 (1949).
[6]A. Abragam and B. Bleaney, *Electron Paramagnetic Resonance of Transition Ions* (Clarendon, Oxford, 1970).
[7]J. M. Baker and F. I. B. Williams, Proc. Phys. Soc. London 78, 1340 (1961).
[8]J. Rosenthal, Phys. Rev. 164, 363 (1967).
[9]D. C. Giori, U. Pozzi, and G. Ruggeri (unpublished).
[10]All the calculations have been performed by means of the CDC 7600 computer located at the Centro Universitario di Calcolo, Bologna, Italy.
[11]J. Rosenthal, R. F. Riley, and U. Ranon, Phys. Rev. 177, 625 (1969).
[12]H. A. Buckmaster and Y. H. Shing, Phys. Status Solidi A 12, 325 (1972).

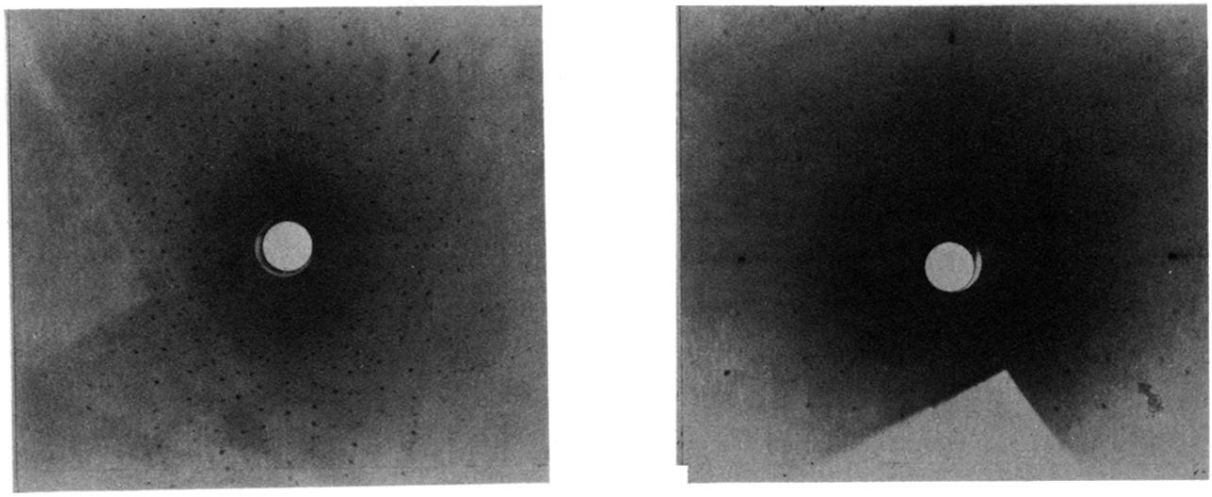

FIG. 2. (a) Transmission and (b) back-reflection photograph of ThOS single crystal. The incident beam is perpendicular to the (001) plane (30-mm specimen-to-film distance).